

# Ferromagnetic spin coupling as the origin of 0.7 anomaly in quantum point contacts

K. Aryanpour and J. E. Han<sup>1</sup>

<sup>1</sup>*Department of Physics, SUNY at Buffalo, Buffalo, NY 14260*

(Dated: October 15, 2019)

We study one-dimensional itinerant electron models with ferromagnetic coupling to investigate the origin of 0.7 anomaly in quantum point contacts. Linear conductance calculations from the quantum Monte Carlo technique for spin interactions of different spatial range suggest that  $0.7 \times (2e^2/h)$  anomaly results from a strong interaction of low-density conduction electrons to ferromagnetic fluctuations formed across the potential barrier. The conductance plateau results due to the strong incoherent scattering at high temperature when the electron traversal time matches the time-scale of dynamic ferromagnetic excitations.

PACS numbers: 73.63.-b, 73.21.-b, 72.10.Di, 73.21.Hb

Quantum point contacts (QPC) are narrow constrictions inside two-dimensional electron gas. They construct one of the building blocks of sub-micrometer devices such as quantum dots and qubits [1, 2]. Dc conductance through a QPC is quantized in steps of  $G_0 = 2e^2/h$  [3, 4] (with  $e$  the charge of an electron and  $h$  Planck's constant). However, experiments also reveal the appearance of an additional shoulder in the conductance measurement near  $0.7G_0$  widely referred to as the *0.7 anomaly* [2]. The origin of 0.7 anomaly in QPC has remained a puzzle over almost a decade. The evolution of the  $0.7G_0$  plateau to  $0.5G_0$  with magnetic field and the enhancement of the  $g$ -factor [2] have strongly suggested that the origin of the anomaly is the electron spin.

A number of scenarios have been proposed, such as spin polarization of the itinerant electrons [5, 6, 7, 8, 9, 10, 11], ferromagnetic correlation [12, 13, 14], formation of a spin 1/2 magnetic moment in the conductance channel [15, 16, 17, 18] and Kondo effect [16, 17, 19], Hubbard-chain [20, 21, 22, 23, 24, 25, 26], Wigner crystallization and anti-ferromagnetism [27]. These approaches have produced a wide range of different phenomenologies, sometimes inconsistent with experiments, and there is no widely accepted microscopic theory to date. The problem is partly due to the approximate methods used in the strongly interacting limit and therefore it becomes essential to perform exact calculations to determine microscopic models which are consistent with experiments. Here we use numerically accurate *Quantum Monte Carlo* (QMC) technique to study the strong correlation effects in the electron transport through a potential barrier.

We find that the 0.7 anomaly at high temperature arises from the incoherent electron scattering from itinerant ferromagnetic fluctuations near the Stoner instability [28], in the strong correlation limit of low electron density created by spatially inhomogeneous gate potential. We show, through a comparison with a model with on-site (short-range) interactions, that the relevant electron scattering is due to the spin fluctuations which are spatially coherent across the potential barrier. With de-

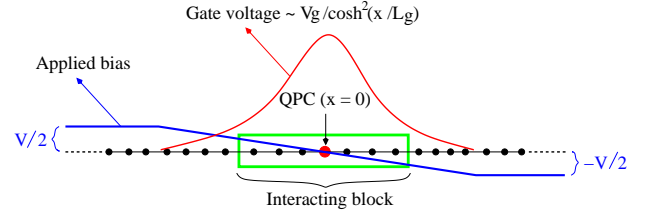


FIG. 1: (Color online) Profile of the 1-D chain with the interacting block (including seven sites in this figure) in the center (QPC). The gate voltage potential  $V(x)$  in Eq.(1) acts as a barrier to control the current flow through the QPC region. A bias with a ramp passing through the QPC is applied across the chain to compute the dc conductance using the Kubo formula in the linear response regime.

creasing temperature, the magnetic excitation becomes slower than the itinerant electrons. The current is then carried by the quasi-particles and the 0.7 plateau gradually disappears. With Zeeman magnetic field, the 0.7 plateau evolves to a robust 0.5 plateau in agreement with experiments.

We model our system using a 1-D electron gas with spin-spin interaction among itinerant electrons as depicted in Fig.1. The Hamiltonian reads

$$\mathcal{H} = \int dx \psi^\dagger(x) \left[ -\frac{\hbar^2}{2m} \frac{\partial^2}{\partial x^2} + V(x) - \mu + \frac{1}{2} \vec{\sigma} \cdot \vec{H} \right] \psi(x) + \int dx [K_1(x) \vec{s}(x) \cdot \vec{s}(x) + K_2(x) \partial_x \vec{s}(x) \cdot \partial_x \vec{s}(x)], \quad (1)$$

with  $\psi(x) = \begin{pmatrix} \psi_\uparrow(x) \\ \psi_\downarrow(x) \end{pmatrix}$  the field operator vector,  $\mu$  the chemical potential,  $\vec{H}$  the Zeeman magnetic field,  $\sigma$  the Pauli matrices and  $V(x)$  the external gate voltage barrier in order to *pinch off* the electron current through the QPC.  $V(x)$  is defined in our model as  $V(x) = V_g / \cosh^2(x/L_g)$  with  $x = 0$  corresponding to the center of the chain,  $L_g$  a characteristic length and  $V_g$  the gate voltage. The operator  $\vec{s}(x) = \psi^\dagger(x) \frac{\vec{\sigma}}{2} \psi(x)$  represents the spin density of itinerant electrons along the chain. Spins interact locally with the coupling constant  $K_1(x) = \alpha(x)K_1$  with  $\alpha(x) = 1 / \cosh(x/L_s)$  an attenuating function with

characteristic length  $L_s$ . We set the spin coupling to smoothly fall off outside of the constriction due to the screening effect by electrons away from the QPC region.  $K_2(x) = \alpha(x)K_2$  is the coefficient of the gradient term accounting for the ferromagnetic Heisenberg interaction. We discretize the continuum model Hamiltonian to a tight-binding chain of lattice constant  $\Delta x$  with the nearest-neighbor hopping  $t$ . Defining  $t = \frac{\hbar^2}{2m\Delta x^2}$ ,  $\mu = \mu - \frac{\hbar^2}{m\Delta x^2}$ ,  $\sqrt{\Delta x} \psi(x_i) = c_i$ ,  $|J_0| = -(\frac{K_1}{\Delta x} + \frac{2K_2}{\Delta x^3})$ ,  $|J_1| = \frac{2K_2}{\Delta x^3}$  and  $\vec{s}_p = c_p^\dagger \frac{\vec{\sigma}}{2} c_p$  the discretized Hamiltonian reads

$$\mathcal{H} = -t \sum_{\langle ij \rangle, \sigma} c_{i\sigma}^\dagger c_{j\sigma} - \sum_{i\sigma} (\mu - V_i + \frac{1}{2}\sigma H) c_{i\sigma}^\dagger c_{i\sigma} - \sum_{p \in \text{block}} (J_0 \alpha_p^2 \vec{s}_p \cdot \vec{s}_p + J_1 \alpha_p \alpha_{p+1} \vec{s}_p \cdot \vec{s}_{p+1}), \quad (2)$$

with  $H$  taken along the  $z$  direction and its coefficient  $\sigma = \pm 1$  being the spin index.  $J_0, J_1 > 0$  are set for ferromagnetic coupling and the index  $p$  runs only within the interacting block in Fig.1 confining the interactions to only the vicinity of the QPC. The discretization is valid since we are in the low-density limit with  $\langle c_{i\sigma}^\dagger c_{i\sigma} \rangle < 1$  inside the interacting block. Using  $m \approx 0.067m_e$  for GaAs and  $\Delta x \approx 20$  nm (experimental QPC length is about 200 nm, roughly  $10\Delta x$  for  $L_g = 4$ ),  $t = 1.4$  meV. Our CPU limitations restrict us to about seven sites inside the interacting block which we have found sufficient for observing the desired physical features.

In our calculations, we modify Eq.(2) by allowing the non-local part of the interaction term to extend beyond nearest neighboring sites. We define the block spin operator  $\vec{S} = \sum_{p \in \text{block}} \alpha_p \vec{s}_p$  and rewrite a new Hamiltonian

$$\mathcal{H} = -t \sum_{\langle ij \rangle, \sigma} c_{i\sigma}^\dagger c_{j\sigma} - \sum_{i\sigma} (\mu - V_i + \frac{1}{2}\sigma H) c_{i\sigma}^\dagger c_{i\sigma} - \sum_{p \in \text{block}} (J_0 - \frac{J_1}{2}) \alpha_p^2 \vec{s}_p \cdot \vec{s}_p - \frac{J_1}{2} \vec{S} \cdot \vec{S}. \quad (3)$$

Compared to Eq.(2), Eq.(3) incorporates stronger spin interaction among all the spins within the interacting block. This modification makes the decoupling scheme in QMC more efficient. Interactions beyond nearest neighbors can be thought of a coarse-grained effective Hamiltonian on the discretized lattice in the low wave-vector limit. The effective interaction results from virtual fluctuations to high momentum states which are excluded in the discretized model and it takes a form similar to the RKKY interaction. Since we are interested in the low-density limit near the pinch-off regime with the effective Fermi wave-vector  $k_{F,\text{eff}}$  inside the constriction approaching zero, the  $k_{F,\text{eff}} R_i$  factor for position  $R_i$  inside the constriction also goes to zero and the effective spin interaction over the interacting block becomes predominantly ferromagnetic.

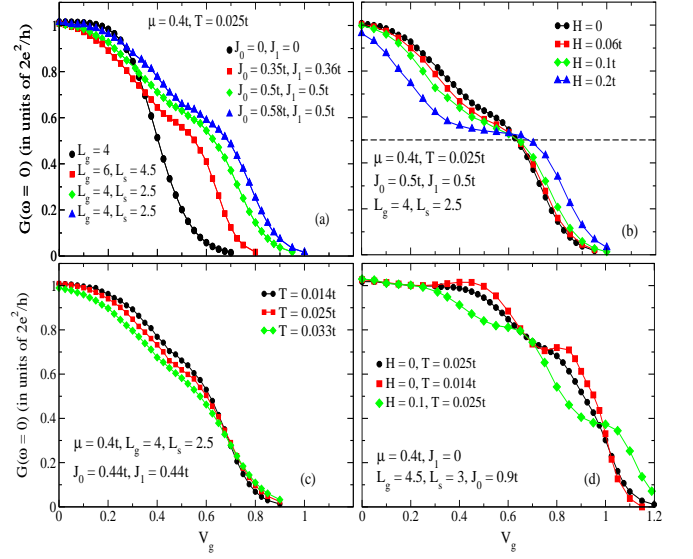


FIG. 2: (Color online) (a) dc conductance as a function of gate voltage  $V_g$  at different values for  $L_g$ ,  $L_s$ ,  $J_0$  and  $J_1$  at  $T = 0.025t$ . Conductance plateaus form at 0.6 – 0.7 times of  $G_0 = 2e^2/h$ . (b) The evolution of the plateau to  $0.5G_0$  as a function of the Zeeman magnetic field. (c) The gradual increase of conductance with decreasing temperature. (d) Purely local model ( $J_1 = 0$ ) as a function of temperature and the Zeeman magnetic field. Local interaction produces qualitatively different transport mechanism from the non-local interaction.

We use a continuous Hubbard-Stratonovich decoupling for the  $\vec{S} \cdot \vec{S}$  term in Eq.(3) and discrete decoupling for local  $\vec{s}_m \cdot \vec{s}_m$  term. We calculate the dc conductance using the Kubo formula in the linear response regime,  $G_{dc}(\omega = 0) = \lim_{\omega \rightarrow 0} \text{Re} i \int_0^\infty e^{i\omega t'} \langle [j(x_j, t'), H'(0)] \rangle dt'$ , where  $j(t') = iet \sum_{\sigma} [c_{1,\sigma}^\dagger(t') c_{0,\sigma}(t') - c_{0,\sigma}^\dagger(t') c_{1,\sigma}(t')]$  is the current operator evaluated at the center of the QPC and  $H'(0) = -e \sum_{m,\sigma} V(x_m) n_{m,\sigma}$  is the external perturbation across the chain with  $V(x_m)$  the normalized source-drain bias with maximum (minimum) voltage 1/2 (–1/2) on the left (right) hand side as depicted in Fig.1. Conductance by the Kubo formula is obtained in terms of the bosonic Matsubara frequencies ( $i\nu_n = \frac{2\pi n}{\beta}$  where  $\beta = 1/k_B T$  with  $k_B$  the Boltzmann constant and positive integer  $n$ ) and it needs to be analytically continued to real frequency to take the dc limit  $G_{dc}(\omega = 0)$ . This task is done by fitting the Matsubara frequency into the Lehmann representation  $G(i\nu_n) = i \int_{-\infty}^\infty d\omega' \frac{\rho(\omega')}{i\nu_n - \omega'}$  with the spectral function  $\rho(\omega)$  as the fitting parameter. After taking the analytic continuation  $i\nu_n \rightarrow \omega + i\eta$ , we obtain the conductance  $G_{dc}(\omega = 0) = \rho(0)$ .

Fig.2(a) plots the dc conductance as a function of the gate voltage  $V_g$  for different values of  $L_g$  and  $L_s$  at several  $J_0$  and  $J_1$  values and fixed chemical potential  $\mu = 0.4t$  when  $H = 0$ . With increasing interaction strength, the plateau evolves from near  $0.5G_0$  [25] to higher val-

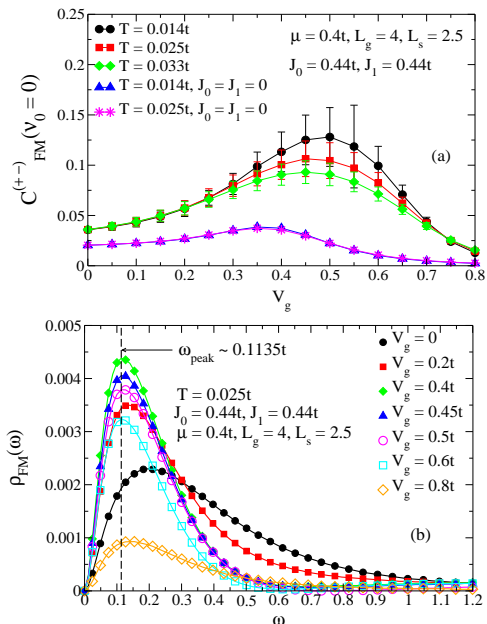


FIG. 3: (Color online) (a) Static ferromagnetic spin correlation function versus the gate voltage at different temperatures. The susceptibility has a strong many-body enhancement (compared to the non-interacting model). (b) Spectral function for dynamic ferromagnetic spin susceptibility  $\rho_{FM}(\omega)$  at different values of gate voltage at  $T = 0.025t$ . The dashed line indicates the excitation frequency.

ues  $0.6 - 0.7G_0$  in the strongly interacting limit with  $J_0, J_1 > \mu$ . Fig.2(b) exhibits the gradual evolution of the plateau near  $0.7G_0$  to  $0.5G_0$  as the Zeeman magnetic field is applied. The significantly wide gate voltage interval for the plateau region ( $\Delta V_g \approx 0.4t$  at  $0.5G_0$  for  $H = 0.2t$ ) compared to the bare Zeeman splitting ( $\Delta V_g = H = 0.2t$ ) is a clear indication for the enhancement of the  $g$ -factor as seen in the experiment[2]. Fig.2(c) shows that, with decreasing temperature  $T$ , the conductance plateau gradually and consistently moves upward with decreasing width. Unfortunately, our current QMC method cannot access temperatures lower than  $T = 0.014t$  due to the phase problem which impairs the statistics. Nevertheless, we are able to capture the correct trend as seen in the experiment for  $0.014t \leq T \leq 0.033t$  and for  $T \gtrsim 0.033t$  the conductance begins to rapidly fall.  $T = 0.025t$  corresponds to  $T \approx 0.41K$ , falling within the experimental range[16]. Features in Fig.2(a)-(c) correctly reproduce the experimental results on the temperature and magnetic field dependence.

Fig.2(d) plots the conductance in the purely local limit ( $J_1 = 0$ ). The local spin model is equivalent to the repulsive Hubbard model [20, 21, 22, 26] with the on-site Coulomb parameter  $U$  given as  $U = 3J_0/4$  by redefining the gate potential  $V_i$  to absorb the one-body terms. Although the local limit produces a well-defined 0.7 feature at zero field, it is inconsistent with the 0.7 phenomenol-

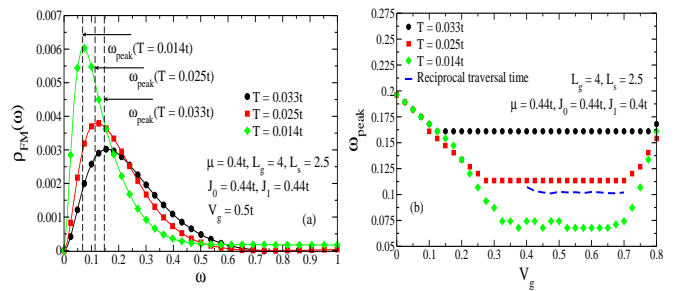


FIG. 4: (Color online) (a)  $\rho_{FM}(\omega)$  at  $V_g = 0.5t$  for different temperatures. The peak frequency  $\omega_{peak}$  corresponds to ferromagnetic excitation energy. (b) The excitation energy as a function of gate voltage  $V_g$  at different temperatures. When the traversal time  $\tau$  (dashed line) is long inside the constriction, *i.e.*  $\omega_{peak}\tau > 1$ , the electron scattering becomes strong and the conductance plateau results.

ogy. First, the 0.7 feature becomes more pronounced as temperature is lowered. Second, more interestingly, at finite magnetic field two plateaus appear with the 0.7 feature shifted to higher conductance and another plateau emerging near  $G \sim 0.3G_0$ . It is very interesting that these results are consistent with the scenario of spin singlet-triplet formation discussed in Refs.[18, 29]. The main difference here is that the spin is self-generated from itinerant electrons in our model, not as an external spin [18] or from a quasi-bound state [29]. Near the pinch-off, electron density and the spin density are low and the spin-singlet does not form and the conductance plateau does not appear at  $H = 0$ . However, at finite  $H$ , the spin moment becomes enhanced enough to produce the spin-singlet conductance plateau.

In the presence of non-local interactions, an itinerant electron interacts with many neighboring sites and the resulting spin multiplets are not necessarily  $S = 0$  or 1. With the finite interacting range, a spatially coherent ferromagnetic state extends over the interacting block at finite  $H$  and becomes harder to be flipped by scattering of an itinerant electron. Therefore, the non-local interaction blocks the minority-spin band and the 0.5 plateau results from spin-splitting, instead of the 0.3-plateau through the singlet formation. It has been shown previously that ferromagnetic coupling beyond local interaction stabilizes the ferromagnetic phase in uniform 1-D chain [14].

Within the constriction near the pinch off, due to the low density of electrons, the ferromagnetic spin correlations are considerably enhanced at low enough  $T$ . We compute the ferromagnetic spin correlation function (FSCF),  $C_{FM}^{(+)}(\nu_n) = \frac{1}{N^2} \sum_{p,m \in block} \int_0^\beta e^{i\nu_n \tau} \langle S_p^+(\tau) S_m^-(0) \rangle d\tau$ , with  $\nu_n = \frac{2\pi n}{\beta}$  ( $n \geq 0$ ) the bosonic Matsubara frequency,  $\tau$  the imaginary time and  $N$  the number of sites inside the interacting block in Fig.1. Fig.3(a) plots the static FSCF ( $\nu_0 = 0$ ) as a function of  $V_g$  at different  $T$  values cor-

responding to the conductance curves in Fig.2(c). In comparison with the non-interacting system, the static FSCF is significantly enhanced as  $T$  is lowered when there is interaction. Enhancement of the static FSCF is effective only around the pinch-off due to the singular nature of the 1-D density of states. The gate voltage range for the maximum enhancement of static FSCF also coincides with that of the plateaus in Fig.2(a)-(c), indicating the effect of strong ferromagnetic correlations on the appearance of the plateau. The dynamic ferromagnetic spin susceptibility can be obtained by analytically continuing the FSCF using the same method employed for the conductance. Through the fluctuation-dissipation theorem,  $\rho_{FM}(\omega)$ , the spectral function for magnetic excitations can be obtained from the analytically continued  $C_{FM}^{+-}(i\nu_n \rightarrow \omega + i\eta)$  from positive  $\nu_n$ . In Fig.3(b),  $\rho_{FM}(\omega)$  has been plotted for different values of  $V_g$  at  $T = 0.025t$  corresponding to Fig.3(a). The height of the peak grows as  $V_g$  increases towards the pinch off, reaching its maximum for  $V_g \approx 0.4t - 0.5t$ , around  $\omega_{peak} \approx 0.1135t$  as indicated by the dashed line. As  $V_g$  is further increased, the height of the peak decreases in agreement to the decrease in the static FSCF in Fig. 3(a). However, the location of the peak continues to stay at  $\omega_{peak} \approx 0.1135t$  as the characteristic excitation energy at  $T = 0.025$  up to  $V_g \approx 0.7t$  where ferromagnetic correlations have almost been obliterated as shown in Fig.3(a).

Tokura and Khaetskii [11] addressed the effect of scattering for electrons in the current due to the local paramagnons as the origin of the 0.7 anomaly in the QPC using the second order perturbation approach with local interactions. Following Büttiker and Landauer in Ref.[30], we argue that magnons, perceived as spin waves with characteristic frequency  $\omega_{peak}$ , can strongly interfere with electrons while transmitting through the gate voltage barrier at frequencies  $\omega_{peak} \sim 1/\tau$  where  $\tau$  is the traversal time for tunneling through the barrier in the absence of magnons defined as  $\int_{x_1}^{x_2} dx \sqrt{\frac{m}{2[V(x)-E]}}$ , with  $x_1$  and  $x_2$  the classical turning points,  $E \approx \mu$  the incident energy and  $V(x) = V_g / \cosh^2(x/L_g)$  the gate voltage barrier.

Fig.4(a) presents  $\rho_{FM}(\omega)$  for  $V_g = 0.5t$  (maximum FSCF in Fig.3(a)) at three different  $T$  values. The characteristic frequency  $\omega_{peak}$  decreases as the temperature is lowered and therefore the spin waves soften at the onset of Stoner instability in the system as explained in detail in Ref.[28]. Fig.4(b) plots  $\omega_{peak}$  as function of  $V_g$  for these three different temperature values along with the reciprocal traversal time  $1/\tau$  (nearly constant as a function of  $V_g$ ). While  $\omega_{peak} \sim 1/\tau$ , strong interference between the spin fluctuations and electrons tunneling through the gate voltage barrier leads to the suppression of the conductance for the gate voltage values in the vicinity of the pinch off. The manifestation of this suppression is the appearance of a plateau in the conductance as a function of the gate voltage near the pinch off. With decreasing

temperature and therefore  $\omega_{peak} \ll 1/\tau$ , as seen in Fig.4(a) and (b) for  $T = 0.014t$ , the itinerant electrons begin to see an effectively static ferromagnetic mean-field and scattering of electrons off magnetic excitations becomes coherent. As a result, the conductance increases and the plateau disappears.

We have demonstrated the incoherent electron scattering due to ferromagnetic spin-spin correlations in a quasi 1-D chain as the underlying physics behind 0.7 anomaly phenomenon in the QPC. We have shown that the non-local Heisenberg spin coupling is important for correct 0.7 phenomenology, compared to the models with local interactions. We thank Jonathan Bird and Igor Žutić for helpful discussions. This project was supported by NSF DMR-0426826 and we acknowledge the CCR at the SUNY Buffalo for computational resources.

- 
- [1] J. Lantz *et al.*, Physica C, **368**, 315 (2002).
  - [2] K. J. Thomas *et al.*, Phys. Rev. Lett. **77**, 135 (1996).
  - [3] B. J. van Wees, *et al.*, Phys. Rev. Lett. **60**, 848 (1988).
  - [4] D. A. Wharam *et al.*, J. Phys. C, **21**, L209 (1988).
  - [5] Chuan-Kui Wang and K.-F. Berggren, Phys. Rev. B. **54**, R14257 (1996); Phys. Rev. B. **57**, 4552 (1998)
  - [6] L. Calmels and A. Gold, Solid State Commun. **106**, 139 (1998)
  - [7] N. Zabala, M. J. Puska, and R. M. Nieminen, Phys. Rev. Lett. **80**, 3336 (1998).
  - [8] H. Bruus, V. V. Cheianov, and K. Flensberg, Physica E, **10**, 97 (2001).
  - [9] D. J. Reilly *et al.*, Phys. Rev. Lett. **89**, 246801 (2002); Phys. Rev. B. **72**, 033309 (2005)
  - [10] A. A. Starikov, I. I. Yakimenko, and K.-F. Berggren, Phys. Rev. B. **67**, 235319 (2003)
  - [11] Y. Tokura, and Khaetskii, Physica E, **12**, 711 (2002).
  - [12] B. Spivak, and F. Zhou, Phys. Rev. B. **61**, 16730 (2000)
  - [13] L. Bartosch, M. Kollar, and P. Kopietz, Phys. Rev. B. **67**, 092403 (2003)
  - [14] K. Yang, Phys. Rev. Lett. **93**, 066401 (2004).
  - [15] T. Rejec and Y. Meir, Nature **422**, 900 (2006).
  - [16] S. M. Cronenwett *et al.*, Phys. Rev. Lett. **88**, 226805 (2002).
  - [17] K. Hirose, Y. Meir, and N. S. Wingreen, Phys. Rev. Lett. **90**, 026804 (2003).
  - [18] V I Puller *et al.*, J. Phys.: Condens. Matter **17** (2005) 5269-5284
  - [19] Y. Meir, K. Hirose, and N. S. Wingreen, Phys. Rev. Lett. **89**, 196802 (2002); J. Phys. : Condens. Matter **20** (2008) 164208
  - [20] S. Kirchner *et al.*, Phys. Rev. B. **59**, 1825 (1999).
  - [21] J. V. Alvarez, and C. Gros, Phys. Rev. Lett. **88**, 077203 (2002); Phys. Rev. B **66**, 094403 (2002).
  - [22] K. Louis, and C. Gros, Phys. Rev. B **68**, 184424 (2003).
  - [23] D. Schmeltzer *et al.*, Phys. Rev. B. **71**, 045429 (2005).
  - [24] A. M. Lunde *et al.*, arXiv:cond-mat/0707.1989v1.
  - [25] C. Sloggett, A. I. Milstein, and O. P. Sushkov, arXiv:cond-mat/0606649v2.
  - [26] O. F. Syljursen, Phys. Rev. Lett. **98**, 166401 (2007).
  - [27] K. A. Matveev, Phys. Rev. Lett. **92**, 106801 (2004); Phys.

- Rev. B. **70**, 245319 (2004).
- [28] S. Doniach, Proc. Phys. Soc. (London) **91**, 86 (1967).
- [29] T. Rejec *et al.*, Phys. Rev. B **62**, 12985 (2000).
- [30] M. Büttiker and R. Landauer, Phys. Rev. Lett. **49**, 1739 (1982).